# The cell wall lipoprotein CD1687 acts as a DNA binding protein during deoxycholate-induced biofilm formation in *Clostridioides difficile*

Emile Auria[a], Lise Hunault[b,c], Patrick England[d], Marc Monot[e], Juliana Pipoli Da Fonseca[e], Mariette Matondo[f], Magalie Duchateau[f], Yannick D.N. Tremblay[g] and Bruno Dupuy[a#]

[a] Institut Pasteur, Université Paris-Cité, UMR-CNRS 6047, Laboratoire Pathogenèse des Bactéries Anaérobies, F-75015 Paris, France
[b] Sorbonne Université, INSERM, CNRS, Centre d'Immunologie et des Maladies Infectieuses (CIMI-Paris), F-75013 Paris, France
[c] Institut Pasteur, Université Paris-Cité, INSERM UMR1222, Unit of Antibodies in Therapy and Pathology, Paris, France
[d] Plateforme de Biophysique Moléculaire, Institut Pasteur, CNRS UMR3528, Paris, France.
[e] Plateforme technologique Biomics, Institut Pasteur, Paris, France
[f] Plateforme Proteomic, Institut Pasteur, France
[g] Department of Biochemistry, Microbiology and Immunology, University of Saskatchewan: Saskatoon, SK, CA

# To whom correspondence should be addressed: BD: Institut Pasteur, Université de Paris cité, UMR-CNRS 6047, Laboratoire Pathogenèse des Bactéries Anaérobies, F-75015 Paris, France
Tel: 33140613175,
Email: bruno.dupuy@pasteur.fr

## Abstract

The ability of bacterial pathogens to establish recurrent and persistent infections is frequently associated with their ability to form biofilms. *Clostridioides difficile* infections have a high rate of recurrence and relapses and it is hypothesised that biofilms are involved in its pathogenicity and persistence. Biofilm formation by *C. difficile* is still poorly understood. It has been shown that specific molecules such as deoxycholate (DCA) or metronidazole induce biofilm formation, but the mechanisms involved remain elusive. In this study, we describe the role of the *C. difficile* lipoprotein CD1687 during DCA-induced biofilm formation. We showed that the expression of *CD1687*, which is part of an operon within the *CD1685-CD1689* gene cluster, is controlled by multiple transcription starting sites and some are induced in response to DCA. Only CD1687 is required for biofilm formation and the overexpression of CD1687 is sufficient to induce biofilm formation. Using RNAseq analysis, we showed that CD1687 affects the expression of transporters and metabolic pathways and we identified several potential binding partners by pull-down assay, including transport-associated extracellular proteins. We then demonstrated that CD1687 is surface exposed in *C. difficile,* and that this localization is required for DCA-induced biofilm formation. Given this localization and the fact that *C. difficile* forms eDNA-rich biofilms, we confirmed that CD1687 binds DNA in a non-specific manner. We thus hypothesize that CD1687 is a component of the downstream response to DCA leading to biofilm formation by promoting interaction between the cells and the biofilm matrix by binding eDNA.

**Keywords**: *Clostridioides difficile*, biofilm, eDNA-binding protein

## Introduction

Gastrointestinal infections are a major public health issue. In high-income countries, the Gram-positive spore forming anaerobe *Clostridioides difficile* is the leading cause of nosocomial diarrhea and colitis in adults receiving antibiotic treatments (1,2). Moreover, *C. difficile* infections (CDI) can be persistent, which is a major challenge in the management of CDI following anti-*C. difficile* antibiotic treatment. Recurrent CDI occur in more than 20% of patients that receive antibiotics to treat their first CDI episode and this rate increases following new episodes (3,4). The causes of recurrences have not been fully elucidated. Recurrence can be caused by either reinfection with a new strain or relapse with the same strain, suggesting that *C*. *difficile* can persist in the gastrointestinal tract (5). Relapses were initially correlated with *C. difficile* ability to sporulate during the infection and resist antibiotic treatment (6,7). However, relapses are also hypothesized to be associated with the persistence of *C. difficile* as a biofilm (8,9). Persistent and chronic infections caused by different pathogens are known to be associated with biofilm formation (10). It is estimated that at least 60% of all nosocomial and chronic bacterial infections are biofilm-associated (11). In support of this hypothesis, *C. difficile* was recently showed to integrate biofilms formed by the colonic microbiota and this biofilm acted as a reservoir for persistence and recurrence in a laboratory model of CDI (9).

Biofilms are structured communities of microorganisms associated with surfaces and encased in a self-produced extracellular matrix, which varies between bacterial species (12). *C. difficile* can form biofilms as a single species or with other bacteria on various abiotic surfaces and several *in vitro* systems (9,13–15). Moreover, *C. difficile* can integrate *in vivo* multi-species communities during a mouse infection, suggesting its ability to integrate mucosal biofilms (16). Additionally, *C. difficile* can form patchy glycan-rich biofilm-like structures in a mono-associated mouse model (17). Although *C. difficile* can integrate multispecies biofilms in the gastrointestinal tract, there is limited knowledge on the biology of *C. difficile* biofilm formation in response to the gastrointestinal environment. During an infection, pathogens encounter

several environmental factors including the presence of antibiotics, bile salts, osmotic pressure and varying nutrient sources and these are known to be important signals for biofilm formation during colonization (18,19). Interestingly, *C. difficile* would face different challenges during dysbiosis as it changes of the nutritional environment, bile salt metabolism, and osmotic and oxidative/nitrosative stresses, (20). Any of these factors could induce biofilm formation. For example, sub-inhibitory concentrations of antibiotics used to treat CDI enhances biofilm formation *in vitro* (21,22). Furthermore, we recently demonstrated that sub-inhibitory concentrations of the secondary bile salt deoxycholate (DCA) enhances *C. difficile* biofilm formation (15). In the DCA-induced biofilm, vegetative cells are protected from the toxicity of DCA as well as antibiotics and antimicrobial peptides (15). We showed that biofilms induced by DCA are formed due to metabolic adaptation and reprogramming that are dependent on the available nutrients and excreted metabolites. Overall, excreted pyruvate is critical for the induction of biofilm formation (23).

In addition to environmental factors inducing biofilm formation, several cellular factors, including cell surface components and regulators, have been shown to influence biofilm formation by *C. difficile* (24). Among the genes that were up-regulated in response to DCA, a gene encoding a lipoprotein (CD1687) is essential for biofilm formation in response to DCA (15). The aim of this study was to characterize the role of CD1687 during biofilm formation by *C. difficile* in response to DCA. We demonstrated that CD1687 is exposed and active at the surface of the bacteria and that it binds DNA *in vitro*. This suggests that CD1687 acts as a protein anchoring the cells to the extracellular DNA (eDNA) present in the biofilm matrix.

## Methods

**Bacterial strains and culture conditions**: Bacterial strains and plasmids used in this study are listed in Table S1 *C. difficile* strains were grown anaerobically (5% H2, 5% CO2, 90% N2)

in TY medium (30g/L tryptone, 20g/L yeast extract) or in BHISG medium (BHI with 0.5% (w/v) yeast extract, 0.01 mg/mL cysteine and 100mM glucose) and supplemented with cefoxitin (250μg/ml), D-cycloserine (8μg/ml) and thiamphenicol (15 μg/ml) when necessary. Additionally, 100ng/mL of anhydrotetracycline (ATC) was added to induce the $P_{tet}$ promoter of pRPF185 vector derivatives in *C. difficile*. *E. coli* strains were grown in LB broth supplemented with chloramphenicol (15μg/mL) and ampicillin (100μg/mL).

**Biofilm assays**: Overnight cultures of *C. difficile* grown in TY medium with appropriate antibiotics were diluted to 1/100 into fresh BHISG containing the desired supplements (240μM DOC, 100ng/mL ATC or both). Depending on the assay, the diluted cultures were then aliquoted either with 1mL per well in 24-well plates (polystyrene tissue culture-treated plates, Costar, USA) or with 200μL in 96-well plates (polystyrene black tissue-culture-treated plates, Greiner Bio One, Austria). The plates were incubated at 37°C in an anaerobic environment for 48h. Biofilm biomass was measured in the 24-well plates using an established method (15). For biofilm assays in 96-well-plates used for microscopy, spent medium was carefully removed by pipetting and 200μL PBS supplemented with 4% of paraformaldehyde (PFA) were added. Plates were incubated for an hour at room temperature and the media was then carefully removed by pipetting before adding PBS for 48h at 4°C. In all assays, sterile medium was used as a negative control and a blank for the assays.

**Gene deletion in *C. difficile***. Gene deletion in *C. difficile* was performed as described in Peltier *et al*. (2020) (25). Regions upstream and downstream of the genes of interest were PCR-amplified using primer pairs described in Table S1. PCR fragments and linearized pDIA6754 (25) were mixed and assembled using Gibson Assembly (NEB, France) and transformed by heat shock in *E. coli* NEB 10β strain. The plasmid constructions were verified by sequencing and plasmids with the right sequences were transformed in *E. coli* HB101 (RP4). The resulting strains were used as donors in a conjugation assay with the relevant *C.*

*difficile* strains. Deletion mutants were then obtained using a counter-selection as described in Peltier et al (2020) (25).

**Protein extraction from *C. difficile* and pull-down assay**. *C. difficile* strains were anaerobically grown for 48h in 20mL BHISG cultures with ATC in tubes. Cells and biofilms were harvested by centrifugation (10 min; 13000 rpm; 4°C) and washed in a cold phosphate buffer (50mM; pH=7.0; 4°C). Cells were then resuspended in 1 ml of the same phosphate buffer containing the purified catalytic domain of the endolysin CD27L (3µg/mL) and suspension was incubated 1h at 37°C to lyse the bacterial cells. The pull-down assay was then performed with Ni-NTA beads as described in supplementary data for CD1687 purification from *E. coli* expression.

**RNA isolation, qRT PCR**: Cells were grown in 24-well plates and 10 wells per plate were used to produce one replicate for one condition. For biofilm conditions, the supernatant was removed by inverting the plate and the biofilms were carefully washed twice then resuspended in 3 mL of PBS. In other conditions, the whole bacterial population was collected and cells were harvested by centrifugation (10 min, 5000 rpm, 4°C) and resuspended in 1 ml of PBS. Cell suspensions in PBS were finally centrifuged (10 min, 5000 rpm, 4°C) and the pellets were frozen at -80°C until further use. Extraction of total RNA from the bacteria and qRT PCR assay were performed as described in Saujet *et al* (2011) (26).

**Whole transcriptome sequencing and analysis**: Transcriptome analysis for each condition was performed using 4 independent RNA preparations. Libraries were constructed using the Illumina Stranded Total RNA Prep Ligation with RiboZero Plus (Illumina, USA) kit. The ribodepletion step was carried using specific probes synthesized specifically to target *C. difficile* ribosomal sequences. After ribodepletion, libraries were prepared according to the

supplier's recommendations. RNA sequencing was performed on the Illumina NextSeq 2000 platform using 67 bases for a target of 10M reads per sample.

**Electromobility shift assays (EMSA)**. Only freshly purified CD1687 from *E. coli* were used in these assays. CD1687 (from 0.5µM to 16µM) was incubated with DNA (pUC9 or PCR product) in 10µl of sodium phosphate buffer (50mM; pH=8.0) for 30 min at room temperature. Samples were loaded and migrated on TAE buffered agarose gels (1% w/v) for 90min at 100V. Controls were performed with CD1687 denatured at 100°C for 15 min before the assay. Gels were stained with ethidium bromide and pictures were taken with an Amersham ImageQuant 800 (Cytiva). The pUC9 plasmid was prepared from *E. coli* stock using the Nucleospin plasmid kit (Macherey-Nagel, Germany) and the PCR amplicon used was generated using *C. difficile* 630*Δerm* as the DNA template and primers targeting the region of *CD1438* (Table S1). gDNA was extracted from cell culture using the DNeasy Blood & Tissue Kit (QIAGEN, Netherlands).

**5'RACE experiment**. A 5'RACE was performed using the 5' RACE System for Rapid Amplification of cDNA Ends, version 2.0 kit (Invitrogen, USA). Briefly, cDNA was generated by reverse transcription from total RNA extract followed by degradation of the RNA. dC-tailing was then performed with the cDNA and the resulting dC-tailed DNA was used as the template in PCR as described in the kit instructions. The PCR products were analyzed by agarose gel electrophoresis (1% agarose in TAE buffer). To identify the transcription start sites, PCR products were inserted into the pGEM-T easy vector kit as described by the manufacturer (Promega, USA). Insert were then PCR-amplified and the resulting PCR products were sequenced.

**Epifluorescence microscopy.** For microscopy, 48h biofilms were generated in 96-well plates (black, Greiner) as described above, washed and 50µl of the polyclonal anti-CD1687 antibodies diluted in PBS (400 ng/mL) was then added to each well and incubated overnight

at 4°C. The wells were carefully washed twice with PBS followed by the addition of a solution containing DAPI (1/1000 dilution) and secondary antibodies (goat anti-rabbit conjugated with Texas Red; 1/5000 dilution; Invitrogen) in PBS. The plates were incubated at room temperature for 2h. Wells were then carefully washed with PBS and 200µl of fresh PBS was added for data acquisition. Images were taken with the Nikon Eclipse Ti inverted microscope (Nikon, Japan).

**Statistical analysis.** The biofilm assays and RT-qPCR were analysed using a one-way ANOVA test followed by either a Tukey's multiple comparison test or a Dunnett's multiple comparison test.

**Data Availability.** RNA-Seq data generated in this study are available in the NCBI-GEO with the accession number GSE218475. The mass spectrometry proteomics data have been deposited to the ProteomeXchange Consortium via the PRIDE partner repository with the dataset identifier PXD038282.

## Results

### Genes of the *CD1685-CD1689* locus form an operon but multiple transcription start site control their expression

In previous transcriptomic experiments, we observed that the majority of genes in the *CD1685 - CD1689* cluster were up-regulated in the 48h DCA-induced biofilm formed by *C. difficile* strain 630Δ*erm* (15,23). However, inactivation of CD1687 but not CD1688 prevented DCA-induced biofilm formation. To verify that the *CD1685-CD1689* genes formed an operon, RT-PCR experiments were performed with RNA extracted from cells grown under biofilm inducing conditions (BHISG with 240µM DCA). We observed a unique transcript spanning *CD1685* to *CD1689* suggesting the presence of at least one polycistronic mRNA at this locus (Fig 1a). We

212 then performed qRT-PCR to confirm that the five genes were up-regulated at 48h in the
213 presence of DCA and only small difference in the fold changes were seen (Fig S1a).
214 When looking at our previous RNAseq experiments, we observed a mapping bias of the
215 sequencing reads favouring CD1687, CD1688 and CD1689 (Fig S1b). Interestingly, recent
216 analyses predicted three transcription starting sites (TSS) for the CD1685-CD1689 locus: one
217 upstream of the *CD1685* gene (TSS1), one upstream the *CD1686* gene (TSS2) and one in the
218 coding sequence of *CD1686* (TSS3) (27,28) (Fig 1c). To confirm the existence of multiple TSS,
219 5'-RACE experiments were performed with total RNA extracted from cells grown for 48h in
220 BHISG with DCA (i.e. biofilm-inducing) or without DCA (i.e. non-biofilm inducing). The initial
221 reverse transcriptions were performed with two primers annealing either the coding sequence
222 of *CD1686* (P1686) or the coding sequence of *CD1687* (P1687) (Fig 1bc). In the absence of
223 DCA, only one amplicon was observed, which is associated with the TSS inside *CD1686.* This
224 amplicon was detectable when the P1686 primer was used but not with the P1687 primer. In
225 the presence of DCA, we observed amplicons corresponding to the three predicted TSS with
226 either primer (P1686 or P1687) and two additional amplicons were detected with P1687. This
227 suggest that these two additional TSS (TSSa and TSSb; Fig 1c) are active in the presence of
228 DCA and one of these (TSSa) appears to be the most active of all TSS (Fig1b). Each amplicon
229 was sequenced (Table S2) and the location of TSS1, TSS2 and TSS3 closely matched their
230 predicted location. However, high variation of the sequences for TSSa and TSSb made it
231 difficult to identify their exact location. Overall, the transcription of the *CD1685-CD1689* operon
232 is initiated from multiple TSS in the presence of DCA, suggesting that multiple factors are
233 integrated to regulate the expression of the CD1685-CD1689 operon to reflect the state of the
234 bacterial population.
235
236 **Overexpressing CD1687 induces biofilm formation in the absence of DCA**
237
238 We previously inactivated *CD1687* using the Clostron system (15) but this approach is known
239 to have some limitations. To confirm that only *CD1687* was required for biofilm formation,

deletion of *CD1686*, *CD1687* and *CD1688-CD1689* were generated (Fig S2a). As observed before, only the deletion of *CD1687* negatively affected biofilm-formation and complementation restore the phenotype (Fig S2bc). Interestingly, deletion of *CD1686* removed TSS3, TSSa and TSSb suggesting that TSS1 and/or TSS2 are sufficient for the transcription of CD1687 in the presence of DCA resulting in biofilm formation.

Since CD1687 is required for DCA-induced biofilm formation and previously localised in the cell wall fraction (15), we hypothesized that CD1687 is a DCA-sensing protein. To test this hypothesis, we verified the ability of CD1687 to directly interact with DCA using surface plasmon resonance. We showed that CD1687 can interact with DCA (Fig S3). However, the dissociation constant is high (Kd of 1.65±0.58mM), and the estimated stoichiometry of the interaction is of 5±1 DCA molecules for one CD1687 protein, which implies that the interaction is not specific.

Interestingly, we observed an increase in biofilm formation in the presence and, to a certain extent, in absence of DCA when the Δ*1687* mutant was complemented with an inducible plasmid-borne CD1687 (pDIA6920) (Fig S2C). Although the increase was not significant, it suggested that CD1687 could induce biofilm formation in the absence of DCA. To test this hypothesis, pDIA6920 was introduced in the wild type strain and its ability to form biofilm in the absence of DCA was evaluated with and without the addition of the inducer ATC. When CD1687 was overexpressed, a stronger biofilm was detectable at 24h and 48h (Fig 2). Taken together, our results suggest that CD1687 expression is critical for biofilm formation which does not require DCA for its activity.

**CD1687 affects the expression of several transporter and metabolic priorities**

As CD1687 is essential for DCA-induced biofilm formation and its overexpression can induce biofilm formation in the absence of DCA, we sought to identify genes controlled by CD1687

during the biofilm formation process. To do so, we performed two transcriptomic analyses: one comparing the wild type and the Δ*1687* mutant grown in presence of DCA for 24h, and the second comparing the wild-type grown in absence of DCA for 24h overexpressing CD1687 or not overexpressing CD1687.

A total of 527 genes had a significant differential expression with a fold change <0.5 or >2 in the wild type strain compared to the Δ*1687* mutant under biofilm inducing conditions (+DCA) (Fig 3). In the presence of DCA, CD1687 seems to mainly downregulate the cell wall reticulation (*vanY2Y3*) as well as several uncharacterized regulators (Fig S4, Table S3). There seems to be a shift in membrane transporters that may result in an increase in the importation of branched-chain amino acids, iron and a change in sugar transport (Table S3). In terms of metabolism, the cells shift from the utilization of succinate (*CD2338-CD2344*), the Wood-Ljungdahl pathway and the biosynthesis of aromatic amino acids to the fermentation of acetoin, leucine, branched chain amino acids and glycine (Fig S4, Table S3).

When CD1687 was overexpressed, 809 genes were differentially expressed, 343 genes were up regulated and 466 were down-regulated (Fig 3). As described in Fig S4, changes in gene expression indicate a shift in transporters, metabolism and regulation. Specifically, the expression of several sugar transporters is increased whereas the expression of the branched chain amino acids, methionine, alanine and glycine transporters is down-regulated (Table S3). In terms of metabolism, genes involved in acetoin utilization, Stickland fermentations involving aromatic amino acids or leucine, the Wood-Ljungdahl pathway and the pentose phosphate pathway are up-regulated as well as those involved in the biosynthesis of several amino acids such as histidine, isoleucine, valine and cysteine (Table S3). The *dltABCD* operon is up-regulated suggesting an increase of the D-alanylation of the teichoic acids (*dltABCD*). Interestingly, we noted that the gene cluster encoding the flagellum and genes associated with sporulation were up-regulated.

When we compared both transcriptomic analyses, few genes overlapped between both analyses. Only 69 genes changed in the same direction whereas 47 genes were regulated in opposite direction (Fig 3). The remaining 1220 genes were differentially expressed only under either condition (Fig 3). The genes that were regulated in both conditions include those involved in cysteine synthesis (*cysE*, *cysK*), leucine utilization in Stickland fermentation (*hadABCI*), acetoin fermentation (*acoABCL*), cell wall proteins (*cwp9*, *cwp12*), some transporters (*alsT* transporting alanine or glycine, *rbsK* transporting ribose) and regulation (*sinRR'*). Overall, this suggests that CD1687 induces metabolic reorganization, including those occurring in response to DCA that leads to biofilm formation (23).

However, these changes do not fully align with our previous analyses (23). We previously observed that DCA causes the up-regulation of gene involved in butanoate, lactate and acetate fermentations, a shift in Stickland fermentations from the use of aromatic amino acids to the use of branched chain amino acids and glycine, and the down-regulation of genes involved in glycolysis, glucose intake and sporulation (23). These changes were not observed when CD1687 was overexpressed suggesting that CD1687 is not involved in those processes or does not mediate the immediate response to DCA. CD1687 is probably part of the downstream response and may interact with other proteins to promote these changes.

**CD1687 interacts with several cell wall proteins**

Given that CD1687 is a cell wall protein (15) and does not have a transmembrane domain, we hypothesized that CD1687 induces transcriptional changes by transmitting external signals by interacting with membrane proteins. To find these potential proteins, we performed a pull-down assay using crude extracts of *C. difficile* cells overexpressing a hexahistidine tagged CD1687 in BHISG without DCA, and 43 proteins were captured (Table S5). Among the identified proteins, four are predicted to be membrane proteins and include a component of sugar

transporter (CD2667) and a sodium symporter (CD2693). We also identified four proteins that belong to the large family of solute binding proteins associated with ABC transporters and one nucleotide phosphodiesterase (CD0689). These five proteins could be involved in signal transport and cellular response leading adaptation in different environmental conditions (29,30). Among the membrane proteins, we also found a putative lipoprotein (CD0747) and a LCP (LytR-CpsA-Psr) family protein (CD2766) involved in the cell wall polysaccharide assembly (31). We noted that only one encoding gene of protein partners (CD0037) was up-regulated in both transcriptomes (Table S5), which is typically localized in the cytoplasm. Since most of the membrane proteins identified by the pull-down experiment are cell wall proteins involved in membrane transport, it is possible that CD1687 directly affect transport of different nutrients and is consistent with the observed effect in our transcriptomes.

**CD1687 is exposed at the cell surface**

Since CD1687 was detected in the cell wall fraction (15), we wondered whether CD1687 is exposed at the cell surface. To verify this, we performed epifluorescence microscopy analysis of *C. difficile* 630Δ*erm* strain and its derivatives using rabbit polyclonal antibodies raised against CD1687. When grown 48 hours in BHISG with or without DCA, no signal was observed in the Δ*1687* mutant confirming the specificity of our antibody (Fig 4 and Fig S5). For the wild-type strain, we observed a weak signal when grown in absence of DCA, confirming that this protein is expressed at low levels under non-biofilm inducing conditions. In the presence of DCA, the signal was stronger in the presence of DCA, although the expression of CD1687 was not homogeneous in the population. In contrast, the signal for CD1687 is homogenous in the population of the complemented Δ*1687* strain (Fig 4 and Fig S5). Since the cells were not permeabilized during the experiment, we concluded that CD1687 is exported to the cell wall and exposed at the cell surface.

Based on the cellular localisation of CD1687, we wondered if the addition of the anti-CD1687 antibodies during growth could prevent DCA-induced biofilm formation. As shown in Fig 5a,

the addition of the anti-CD1687 polyclonal antibodies to cells grown under biofilm inducing conditions (BHISG + 240µM DCA) strongly inhibited biofilm formation in a dose-dependent manner. No inhibitory effect was observed when an unpublished non-specific antibody was used at the highest concentration of anti-CD1687 that inhibited biofilm formation (data not shown). Additionally, bacterial growth was unaffected by the antibodies, regardless of the concentration used in the biofilm assays (Fig 5b). Therefore, inhibiting extracellular function of CD1687 prevents biofilm formation, suggesting that the presence of the CD1687 at the surface of the cell wall is critical for DCA-induced biofilm formation.

To get some insights on the structure-function of CD1687, we used the software AlphaFold2 (32) to predict the 3D protein structure of CD1687. As shown in Fig 5c, CD1687 has an alpha helix N-terminal signal peptide and two putative beta domains. To search for possible functions of the beta barrels, the putative structure of CD1687 was analysed in the Ekhidna database through the Dali server (33), but no function was detected. Since the function of CD1687 could be assigned to one of the two beta domains, we complemented the Δ*1687* mutant by overexpressing CD1687 with either one of the two domains removed and growing these strains under biofilm inducing conditions (BHISG + 240µM DCA. Complementation of the mutant was not observed, indicating that *C. difficile* needs both beta domainds of the CD1687 to form DCA-induced biofilms (Fig 5d).

**CD1687 binds to DNA in a non-specific manner**

Since we did not identify a potential function from the CD1687 structure, we sought to determine if CD1687 has a DNA-binding activity as observed for *Staphylococcus aureus* lipoproteins that promote eDNA-dependent biofilm formation (34). Since the *C. difficile* biofilm matrix is mainly composed of eDNA (15), we tested the ability of CD1687 to bind to DNA by performing an electromobility shift assay (EMSA). When the purified CD1687 protein was incubated with the *E. coli* DNA plasmid pUC9 or a PCR-generated amplicon produced from *C. difficile* DNA (from a sequence in the region of *CD1438*), we observed that the migration of the

379 DNA was shifted by the presence of the CD1687 and increasing CD1687 concentration
380 correlates with more retention (Fig 6ab). However, we did not observe a shift when CD1687 is
381 heat-inactivated or if BSA was used as control at the highest concentration of CD1687 that
382 shift DNA fragments. Therefore, CD1687 can bind DNA and could potentially interact with
383 eDNA when exposed at the surface.
384

385 ## Discussion

386

387 In this study, we confirmed that only CD1687 in the *CD1685-CD1689* cluster was required for
388 DCA-induced biofilm formation and this required the localization of CD1687 at the cell surface.
389 Despite this importance, there is a significant heterogeneity in response to DCA for the
390 expression and localization of CD1687 at cell surface in the population as observed by
391 microscopy (Fig 4 and Fig S5). This would explain the relatively low transcriptional level of the
392 *CD1685-CD1689* gene cluster at the population level (15). Interestingly, the more CD1687 is
393 homogeneously expressed in the cell population, the greater the biofilm formed (Fig 4, Fig
394 S2c). To our knowledge, expression heterogeneity of critical biofilm components has not yet
395 been reported in *C. difficile*. Phenotypic heterogeneity in biofilms is well characterized in
396 several other bacterial species resulting in phenotypic diversification and division of labor in a
397 clonal bacterial population (35). For example, a subpopulation of cells synthesize the
398 exopolysaccharides matrix during biofilm formation in *B. subtilis* (36). Phenotypic
399 heterogeneity has been described in planktonic cells of *C. difficile* and this affected the
400 expression of the flagellum and toxins (37). In this case, heterogeneity is controlled by a
401 specific DNA recombination event mediated by RecV (38) and the Rho factor (39). In addition,
402 *C. difficile* colony morphology is also subjected to phenotypic heterogeneity resulting in
403 changes in bacterial physiology and pathogenesis and this occurs through phase variation of
404 the CmrRST signal transduction system expression (40,41).
405

406 Given that CD1687 forms an operon with a two-component regulatory system (CD1688-1689)
407 and that CD1687 is a cell wall protein, we first hypothesized that CD1687 was involved in
408 signal transduction leading to transcriptional modifications in response of DCA. However,
409 CD1687 did not bind DCA, which eliminates the role of CD1687 as a DCA sensing protein.
410 Furthermore, we compared genes regulated by CD1688 (42) and, with the exception of
411 sporulation, found limited overlap suggesting that CD1687 may not be part of the CD1688-
412 CD1689 signaling cascade. This is consistent with the absence of CD1689 and CD1688 in our
413 pull-down assay. However, several solute-binding proteins and transporter-associated
414 proteins were isolated in a pull-down assay. This and the transcriptional analysis provide
415 evidence that CD1687 influences the metabolism of *C. difficile*. In support of this, regulators
416 (Spo0A, CodY and SinRR') that manage metabolic priorities during growth phases, were
417 differentially regulated when CD1687 was overexpressed (26,43,44). Furthermore, the
418 expression of the gene encoding toxin and those involved in sporulation were also affected
419 and these processes are known to be dependent on the metabolic state of *C. difficile*. When
420 we compared the genes differentially regulated in the absence of CD1687 under DCA-inducing
421 conditions to those differentially regulated when CD1687 was overexpressed in the absence
422 of DCA, there were only 69 common genes, which included genes involved in different
423 metabolic pathways and transport. However, these changes in metabolism-associated genes
424 did not overlap with our previous analyses on gene expression during DCA-induced biofilm
425 formation (23), suggesting that CD1687 is not part of the immediate response to DCA and
426 probably plays a role in the downstream response. Taken together, our data suggest that
427 CD1687 helps reorganize metabolic priorities in response to DCA but this hypothesis alone
428 does not explain the role of CD1687 in the biofilm formation without DCA. Therefore, CD1687
429 may have additional roles.
430
431 Interestingly, many proteins found at the bacterial cell surface interact with eDNA found in the
432 biofilm matrix and this contributes to the organization and structural stability of the biofilm (45).
433 Membrane lipoproteins have already been shown to directly interact with eDNA and participate

in biofilm architecture. In *S. aureus*, several membrane-attached lipoproteins interacting with the eDNA of the biofilm matrix have been identified as promoting *S. aureus* biofilm formation (34). We demonstrated that CD1687 interacts with DNA in a non-specific manner supporting the hypothesis that CD1687 acts as an eDNA binding protein during biofilm formation by creating anchor points for eDNA on the cell surface. Similar to our observation with CD1687, overexpressing eDNA-binding proteins in *S. aureus* resulted in an increased retention of surface eDNA and an enhanced biofilm biomass. However, deleting the *S. aureus* lipoproteins had minimal impact on biofilm formation but biofilm porosity increase indicating that interactions of the lipoprotein with eDNA contribute to overall biofilm structure. Unlike the lipoprotein found in *S. aureus*, a deletion or inactivation of *CD1687* abolished biofilm formation (34). CD1687 interacting with eDNA seems to be an essential part of DCA-induced biofilm formation. Other structures may also interact with eDNA. Recently, two minor subunits (PilW and PilJ) of the *C. difficile* T4P were shown to directly interact with eDNA to promote biofilm formation (46). Neither subunit have a predicted DNA-binding motif as observed with CD1687. The T4P is a structure that promotes biofilm formation in the absence (47,48) or presence of DCA (23). In the presence of DCA, PilW is upregulated but is not required for biofilm formation (15,23). Furthermore, the *pilW* gene was differently regulated in our transcriptome; up-regulated in the WT vs *Δ1687* with DCA analysis (significantly but below the threshold) and down-regulated in the overexpressed CD1687 vs WT without DCA analysis. Therefore, CD1687 and the T4P may have complementary role and the lack of eDNA-binding by one of these components may change the behavior of *C. difficile* during biofilm formation.

Despite the potential role of CD1687 as an eDNA-binding protein and in metabolism, we cannot exclude that the overexpression of CD1687 modifies the properties of the cell wall through the interactions of CD1687 with other membrane proteins and transporters (Table S5). These interactions could be detected by different sensors, which would activate a feedback loop to modify the cell wall and the composition of the cell surface proteins. For example, the *dltABCD* operon was up-regulated when CD1687 was overexpressed in the absence of DCA. The

462 DltABCD proteins are responsible for the D-alanylation of teichoic acids, which changes the
463 electrical charges of the cell wall and surface (49). Overexpression of CD1687 also affected
464 cell morphology; in response to DCA, cells expressing high levels of CD1687 show reduced
465 size and shape distortion (Fig 4 and Fig S5). Overall, the overexpression of CD1687 may have
466 downstream effects on the physiology of *C. difficile* and these changes may contribute to
467 biofilm formation.
468
469 Finally, our hypothesis is that the mechanism for biofilm formation in the presence of DCA is
470 different than the mechanism when DCA is absent and CD1687 is overexpressed. In the
471 presence of DCA, we know that *C. difficile* goes through a metabolic re-organization (23) and,
472 based on our data, CD1687 would help with metabolic priorities for long term adaptation. Once
473 there is enough eDNA, CD1687 would interact with eDNA binding and serve as an anchor
474 point. When CD1687 is overexpressed independently of DCA, it increases homogeneity of
475 CD1687 surface localization in the population and serves as multiple anchoring sites for eDNA
476 resulting in a strongly adherent biofilm. As observed in *S. aureus*, other lipoproteins may bind
477 eDNA in *C. difficile* and several are upregulated in response to DCA (23). Unlike the
478 lipoproteins characterized in *S. aureus*, the lipoprotein CD1687 probably has a critical function
479 in metabolism in response to DCA and other lipoproteins do not provide functional redundancy.
480 This highlights the importance of CD1687 in promoting biofilm formation. More research will
481 be needed to understand the role and the contribution of these other lipoproteins to biofilm.
482
483 **Acknowledgements**
484 This work was funded by the Institut Pasteur, the “Integrative Biology of Emerging Infectious
485 Diseases” (LabEX IBEID) funded in the framework of the French Government’s “Programme
486 Investissements d’Avenir” and The ANR DifBioRel AAPCE5. EA is a doctoral fellow of
487 Université Paris-Cité. LH is a doctoral fellow of Sorbonne Université.
488
489 **Competing Interests:** The authors declare that there are no competing interests.

## References

1. Rupnik M, Wilcox MH, Gerding DN. *Clostridium difficile* infection: new developments in epidemiology and pathogenesis. Nat Rev Microbiol. 2009 Jul;7(7):526–36.

2. Giles J, Roberts A. Chapter Seven - *Clostridioides difficile*: Current overview and future perspectives. In: Donev R, editor. Advances in Protein Chemistry and Structural Biology [Internet]. Academic Press; 2022 [cited 2022 Sep 20]. p. 215–45. (Immunotherapeutics; vol. 129). Available from: https://www.sciencedirect.com/science/article/pii/S1876162321000845

3. Barbut F, Richard A, Hamadi K, Chomette V, Burghoffer B, Petit JC. Epidemiology of Recurrences or Reinfections of *Clostridium difficile*-Associated Diarrhea. J Clin Microbiol. 2000 Jun;38(6):2386–8.

4. Guery B, Galperine T, Barbut F. *Clostridioides difficile* : diagnosis and treatments. BMJ. 2019 Aug 20;l4609.

5. Sachsenheimer FE, Yang I, Zimmermann O, Wrede C, Müller L v., Gunka K, et al. Genomic and phenotypic diversity of *Clostridium difficile* during long-term sequential recurrences of infection. International Journal of Medical Microbiology. 2018 Apr 1;308(3):364–77.

6. Deakin LJ, Clare S, Fagan RP, Dawson LF, Pickard DJ, West MR, et al. The *Clostridium difficile* spo0A gene is a persistence and transmission factor. Infect Immun. 2012 Aug;80(8):2704–11.

7. Castro-Córdova P, Mora-Uribe P, Reyes-Ramírez R, Cofré-Araneda G, Orozco-Aguilar J, Brito-Silva C, et al. Entry of spores into intestinal epithelial cells contributes to recurrence of *Clostridioides difficile* infection. Nat Commun. 2021 Feb 18;12(1):1140.

8. Tijerina-Rodríguez L, Villarreal-Treviño L, Morfín-Otero R, Camacho-Ortíz A, Garza-González E. Virulence Factors of *Clostridioides* (*Clostridium*) *difficile* Linked to Recurrent Infections. Can J Infect Dis Med Microbiol. 2019;2019:7127850.

9. Normington C, Moura IB, Bryant JA, Ewin DJ, Clark EV, Kettle MJ, et al. Biofilms harbour *Clostridioides difficile*, serving as a reservoir for recurrent infection. npj Biofilms and Microbiomes. 2021 Feb 5;7(1):1–10.

10. Hall-Stoodley L, Stoodley P. Evolving concepts in biofilm infections. Cellular Microbiology. 2009;11(7):1034–43.

11. Jamal M, Ahmad W, Andleeb S, Jalil F, Imran M, Nawaz MA, et al. Bacterial biofilm and associated infections. Journal of the Chinese Medical Association. 2018 Jan 1;81(1):7–11.

12. Vlamakis H, Chai Y, Beauregard P, Losick R, Kolter R. Sticking together: building a biofilm the *Bacillus subtilis* way. Nat Rev Microbiol. 2013 Mar;11(3):157–68.

13. Vuotto C, Donelli G, Buckley A, Chilton C. *Clostridium difficile* Biofilm. In: Mastrantonio P, Rupnik M, editors. Updates on *Clostridium difficile* in Europe: Advances in Microbiology, Infectious Diseases and Public Health Volume 8 [Internet]. Cham: Springer International Publishing; 2018 [cited 2019 Oct 9]. p. 97–115. (Advances in Experimental Medicine and Biology). Available from: https://doi.org/10.1007/978-3-319-72799-8_7

14. Poquet I, Saujet L, Canette A, Monot M, Mihajlovic J, Ghigo JM, et al. *Clostridium difficile* Biofilm: Remodeling Metabolism and Cell Surface to Build a Sparse and Heterogeneously Aggregated Architecture. Front Microbiol. 2018;9:2084.

15. Dubois T, Tremblay YDN, Hamiot A, Martin-Verstraete I, Deschamps J, Monot M, et al. A microbiota-generated bile salt induces biofilm formation in *Clostridium difficile*. NPJ Biofilms Microbiomes. 2019;5:14.

16. Semenyuk EG, Poroyko VA, Johnston PF, Jones SE, Knight KL, Gerding DN, et al. Analysis of Bacterial Communities during *Clostridium difficile* Infection in the Mouse. Infect Immun. 2015 Nov;83(11):4383–91.

17. Soavelomandroso AP, Gaudin F, Hoys S, Nicolas V, Vedantam G, Janoir C, et al. Biofilm Structures in a Mono-Associated Mouse Model of *Clostridium difficile* Infection. Front Microbiol [Internet]. 2017 Oct 25 [cited 2020 Nov 17];8. Available from: https://www.ncbi.nlm.nih.gov/pmc/articles/PMC5661025/

18. Ahmed NA, Petersen FC, Scheie AA. AI-2/LuxS is involved in increased biofilm formation by *Streptococcus intermedius* in the presence of antibiotics. Antimicrob Agents Chemother. 2009 Oct;53(10):4258–63.

19. Krzyściak W, Jurczak A, Kościelniak D, Bystrowska B, Skalniak A. The virulence of *Streptococcus mutans* and the ability to form biofilms. Eur J Clin Microbiol Infect Dis. 2014 Apr;33(4):499–515.

20. Aguirre AM, Sorg JA. Gut associated metabolites and their roles in *Clostridioides difficile* pathogenesis. Gut Microbes. 2022 Dec;14(1):2094672.

21. Đapa T, Unnikrishnan M. Biofilm formation by *Clostridium difficile*. Gut Microbes. 2013 Sep 28;4(5):397–402.

22. Vuotto C, Moura I, Barbanti F, Donelli G, Spigaglia P. Subinhibitory concentrations of metronidazole increase biofilm formation in *Clostridium difficile* strains. Pathog Dis. 2016 Mar;74(2).

23. Tremblay YDN, Durand BAR, Hamiot A, Martin-Verstraete I, Oberkampf M, Monot M, et al. Metabolic adaption to extracellular pyruvate triggers biofilm formation in *Clostridioides difficile*. ISME J. 2021 Jun 21;

24. Meza-Torres J, Auria E, Dupuy B, Tremblay YDN. Wolf in Sheep's Clothing: *Clostridioides difficile* Biofilm as a Reservoir for Recurrent Infections. Microorganisms. 2021 Sep 10;9(9):1922.

25. Peltier J, Hamiot A, Garneau JR, Boudry P, Maikova A, Hajnsdorf E, et al. Type I toxin-antitoxin systems contribute to the maintenance of mobile genetic elements in *Clostridioides difficile*. Communications Biology. 2020 Nov 27;3(1):1–13.

570 26. Saujet L, Monot M, Dupuy B, Soutourina O, Martin-Verstraete I. The key sigma factor of
571 transition phase, SigH, controls sporulation, metabolism, and virulence factor expression
572 in *Clostridium difficile*. J Bacteriol. 2011 Jul;193(13):3186–96.

573 27. Soutourina O, Dubois T, Monot M, Shelyakin PV, Saujet L, Boudry P, et al. Genome-
574 Wide Transcription Start Site Mapping and Promoter Assignments to a Sigma Factor in
575 the Human Enteropathogen *Clostridioides difficile*. Front Microbiol. 2020;11:1939.

576 28. Fuchs M, Lamm-Schmidt V, Sulzer J, Ponath F, Jenniches L, Kirk JA, et al. An RNA-
577 centric global view of *Clostridioides difficile* reveals broad activity of Hfq in a clinically
578 important gram-positive bacterium. PNAS [Internet]. 2021 Jun 22 [cited 2021 Oct
579 11];118(25). Available from: https://www.pnas.org/content/118/25/e2103579118

580 29. Hosie AHF, Allaway D, Jones MA, Walshaw DL, Johnston AWB, Poole PS. Solute-
581 binding protein-dependent ABC transporters are responsible for solute efflux in addition
582 to solute uptake. Molecular Microbiology. 2001;40(6):1449–59.

583 30. Matilla MA, Ortega Á, Krell T. The role of solute binding proteins in signal transduction.
584 Comput Struct Biotechnol J. 2021;19:1786–805.

585 31. Stefanović C, Hager FF, Schäffer C. LytR-CpsA-Psr Glycopolymer Transferases:
586 Essential Bricks in Gram-Positive Bacterial Cell Wall Assembly. Int J Mol Sci. 2021 Jan
587 18;22(2):E908.

588 32. Jumper J, Evans R, Pritzel A, Green T, Figurnov M, Ronneberger O, et al. Highly
589 accurate protein structure prediction with AlphaFold. Nature. 2021 Aug;596(7873):583–9.

590 33. Holm L. Dali server: structural unification of protein families. Nucleic Acids Research.
591 2022 Jul 5;50(W1):W210–5.

592 34. Kavanaugh JS, Flack CE, Lister J, Ricker EB, Ibberson CB, Jenul C, et al. Identification
593 of Extracellular DNA-Binding Proteins in the Biofilm Matrix. mBio. 2019;10(3):e01137-19.

594 35. Stewart WD, Haystead A, Pearson HW. Nitrogenase activity in heterocysts of blue-green
595 algae. Nature. 1969 Oct 18;224(5216):226–8.

596 36. Vlamakis H, Aguilar C, Losick R, Kolter R. Control of cell fate by the formation of an
597 architecturally complex bacterial community. Genes Dev. 2008 Apr 1;22(7):945–53.

598 37. Anjuwon-Foster BR, Maldonado-Vazquez N, Tamayo R. Characterization of Flagellum
599 and Toxin Phase Variation in *Clostridioides difficile* Ribotype 012 Isolates. J Bacteriol.
600 2018 Jul 15;200(14):e00056-18.

601 38. Anjuwon-Foster BR, Tamayo R. A genetic switch controls the production of flagella and
602 toxins in *Clostridium difficile*. PLoS Genet. 2017 Mar;13(3):e1006701.

603 39. Trzilova D, Anjuwon-Foster BR, Torres Rivera D, Tamayo R. Rho factor mediates
604 flagellum and toxin phase variation and impacts virulence in *Clostridioides difficile*. PLoS
605 Pathog. 2020 Aug;16(8):e1008708.

606 40. Garrett EM, Sekulovic O, Wetzel D, Jones JB, Edwards AN, Vargas-Cuebas G, et al.
607 Phase variation of a signal transduction system controls *Clostridioides difficile* colony
608 morphology, motility, and virulence. PLoS Biol. 2019 Oct;17(10):e3000379.

609 41. Garrett EM, Mehra A, Sekulovic O, Tamayo R. Multiple Regulatory Mechanisms Control
610 the Production of CmrRST, an Atypical Signal Transduction System in *Clostridioides*
611 *difficile*. mBio. 2022 Feb 15;e0296921.

612 42. Kempher ML, Morris SC, Shadid TM, Menon SK, Ballard JD, West AH. Response
613 Regulator CD1688 Is a Negative Modulator of Sporulation in *Clostridioides difficile*. J
614 Bacteriol. 204(8):e00130-22.

615 43. Purcell EB, McKee RW, Courson DS, Garrett EM, McBride SM, Cheney RE, et al. A
616 Nutrient-Regulated Cyclic Diguanylate Phosphodiesterase Controls *Clostridium difficile*
617 Biofilm and Toxin Production during Stationary Phase. Infect Immun. 2017;85(9).

618 44. Girinathan BP, Ou J, Dupuy B, Govind R. Pleiotropic roles of *Clostridium difficile* sin
619 locus. PLoS Pathog [Internet]. 2018 Mar 12 [cited 2021 Mar 3];14(3). Available from:
620 https://www.ncbi.nlm.nih.gov/pmc/articles/PMC5864091/

621 45. Campoccia D, Montanaro L, Arciola CR. Extracellular DNA (eDNA). A Major Ubiquitous
622 Element of the Bacterial Biofilm Architecture. Int J Mol Sci. 2021 Aug 23;22(16):9100.

623 46. Ronish LA, Sidner B, Yu Y, Piepenbrink KH. Recognition of extracellular DNA by type IV
624 pili promotes biofilm formation by *Clostridioides difficile*. Journal of Biological Chemistry.
625 2022 Sep 3;102449.

626 47. Maldarelli GA, Piepenbrink KH, Scott AJ, Freiberg JA, Song Y, Achermann Y, et al. Type
627 IV pili promote early biofilm formation by *Clostridium difficile*. Pathog Dis. 2016;74(6).

628 48. Allen R, Rittmann BE, Curtiss R. Axenic Biofilm Formation and Aggregation by
629 *Synechocystis sp.* Strain PCC 6803 Are Induced by Changes in Nutrient Concentration
630 and Require Cell Surface Structures. Appl Environ Microbiol. 2019 Apr 1;85(7):e02192-
631 18.

632 49. Wood BM, Santa Maria JP, Matano LM, Vickery CR, Walker S. A partial reconstitution
633 implicates DltD in catalyzing lipoteichoic acid d-alanylation. J Biol Chem. 2018 Nov
634 16;293(46):17985–96.

635

636

637

638

## Figures

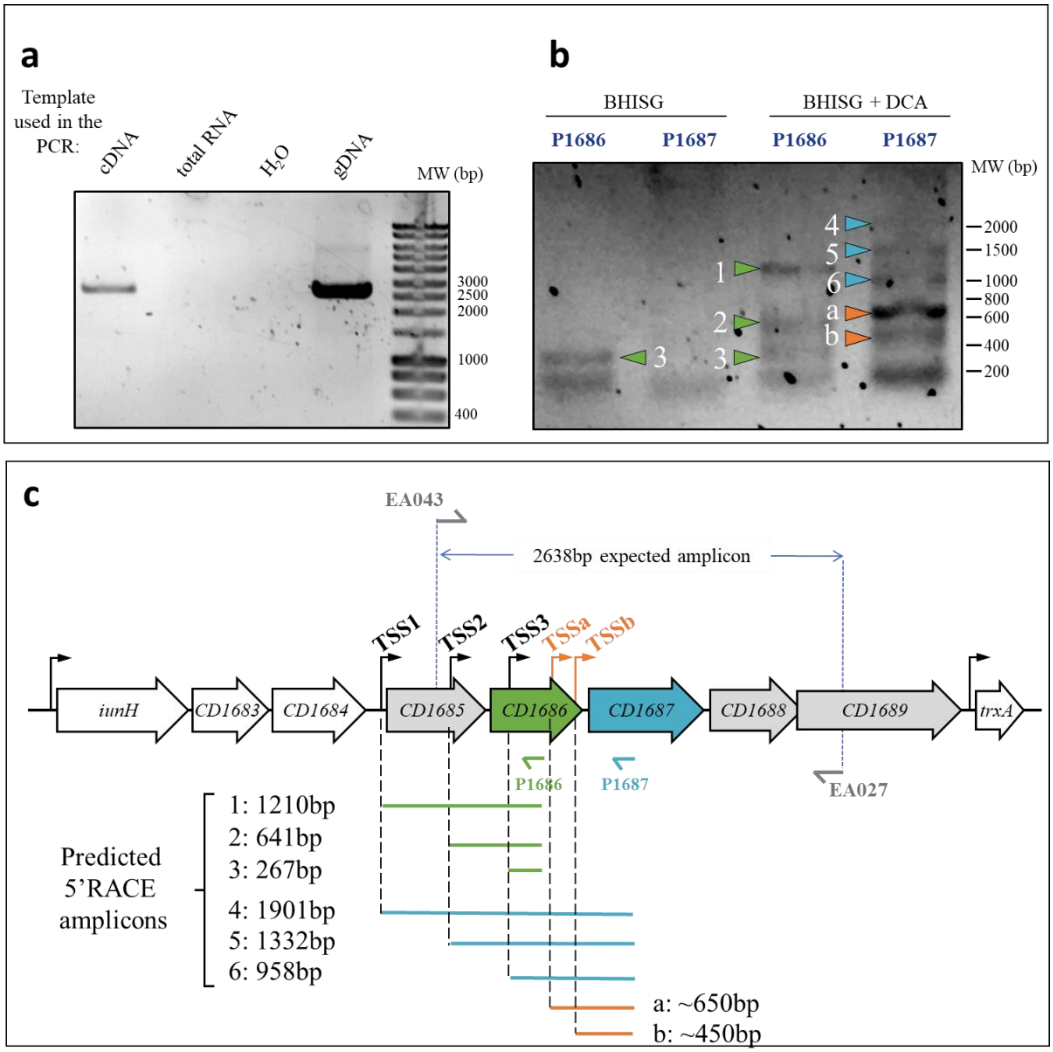


**Figure 1: The *CD1685-CD1689* cluster in *C. difficile* strain 630Δ*erm* forms an operon with multiple transcription start sites**. **a.** RT-PCR performed with primers EA043 and EA027 (Table S1) from various nucleic acid templates. cDNA was obtained using the EA027 primer with total RNA extracted from 48h biofilms grown in BHISG supplemented with DCA (240µM). **b.** 5'RACE results from amplification of the poly-guanylated cDNA obtained respectively with the EA021 and EA018 primers (Table S1), then the P1686 or P1687 primers along with the universal amplification primer (AAP) from the 5'RACE kit. The RNA was extracted from 48h cell cultures grown under biofilm inducing conditions (BHISG + 240µM DCA) or non-biofilm-inducing conditions (BHISG). **c**. Organisation of the *CD1685-CD1689* cluster, the location of the primers used for RT-PCR and the amplicons from the 5'RACE results using the P1686 or P1687 primers (amplicon sizes were predicted from the TSS identified by Soutourina *et al.* (2020) and Fuchs *et al.* (2021). TSS: Transcriptional Start Site; cDNA: complementary DNA; gDNA: genomic DNA.

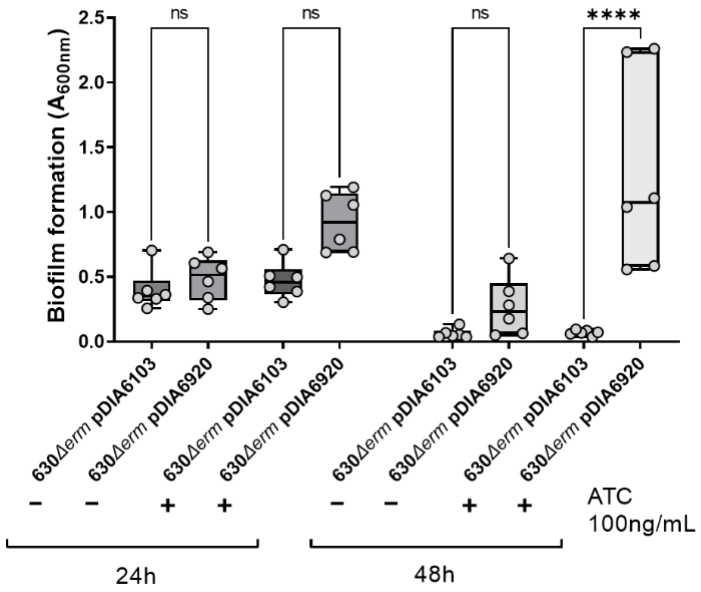


**Figure 2: Overexpression of CD1687 induces biofilm formation in the absence of DCA**. Biofilms formation was assayed 24h or 48h after inoculation in BHISG +/- ATC (100ng/mL) with the wild type strain (630Δ*erm*) containing either a control empty vector (pDIA6103) or the vector allowing the expression of CD1687 under the inducible $P_{tet}$ promoter (pDIA6920). Each data point represents an independent biological replicate composed of 2 to 4 technical replicates.

Asterisks indicate statistical significance with a one-way ANOVA test followed by a Tukey's multiple comparison test (ns: not significant; ****: p<0.0001).

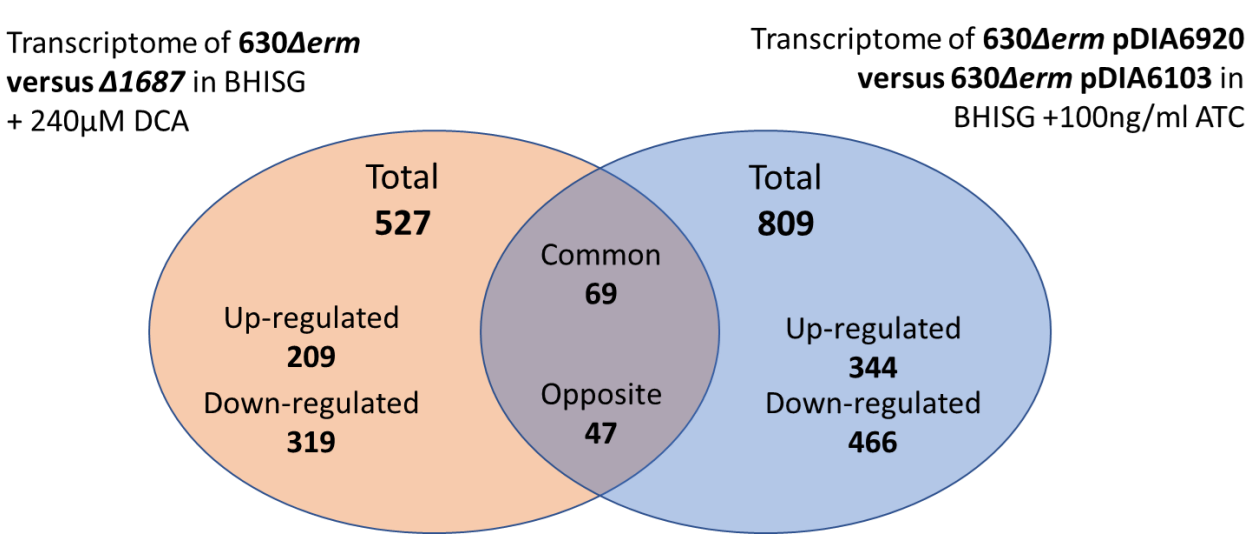


**Figure 3: Differences in gene expression in the two transcriptomics experiments**. Venn diagram of the genes differentially regulated in the two transcriptomics experiments performed in this study (Table S4).

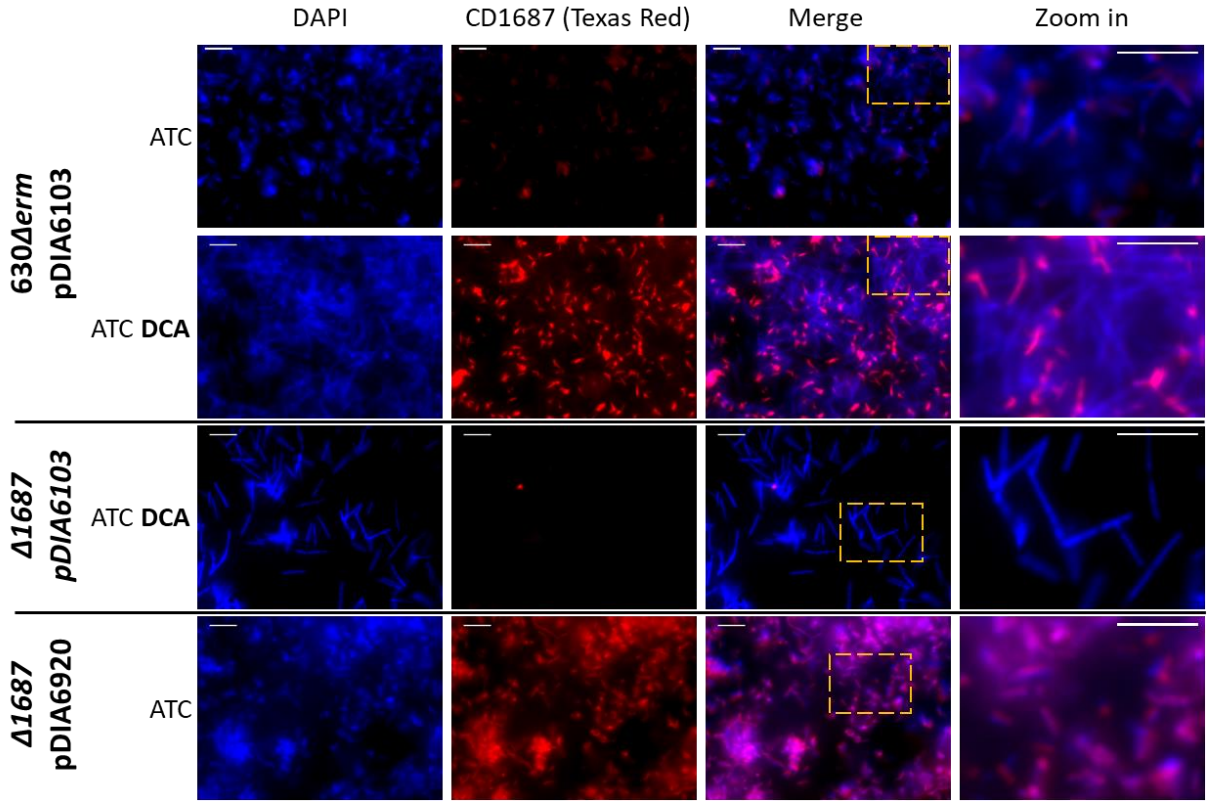


**Figure 4: CD1687 localizes at the cell surface of *C. difficile* and displays heterogenous distribution within the biofilm**. *In situ* epifluorescence microscopy analysis was performed on 48h biofilms grown in BHISG + ATC (100ng/mL) either in the presence or absence of DCA (240µM) as indicated. The strains tested were the wild type strain (630Δ*erm*) carrying the control vector pDIA6103 and with the *Δ1687* strain carrying the plasmid with an inducible CD1687 (pDIA6920) or the control plasmid (pDIA6103). DNA is stained with DAPI (blue) and CD1687 is labelled with specific anti-CD1687 rabbit antibodies detected with a TexasRed-conjugated goat anti-rabbit antibody (red). Pictures are representative of three biological replicates and were taken with a Nikon Eclipse Ti inverted microscope (Nikon, Japan). Scale bar: 10µm.

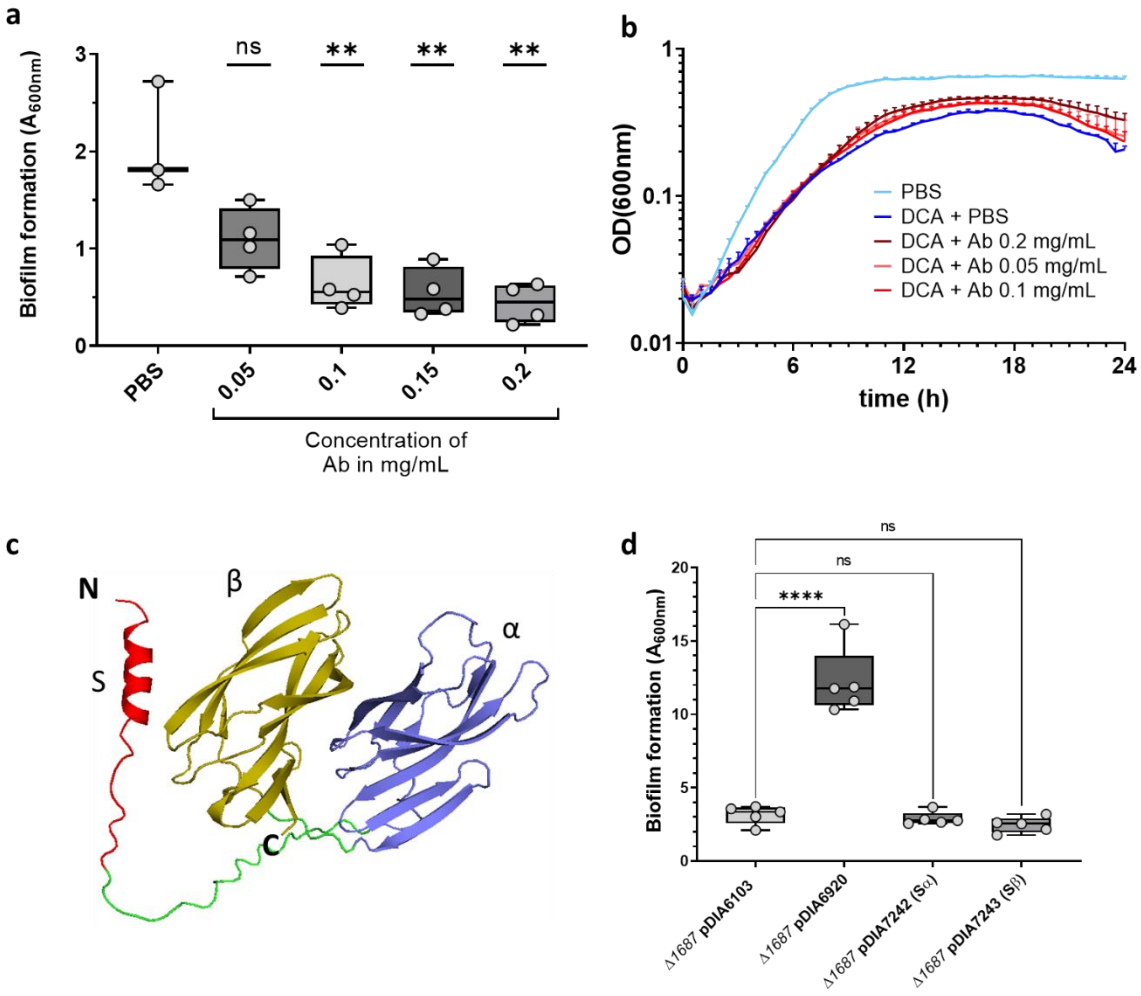


**Figure 5: DCA-induced biofilm formation is inhibited in the presence of anti-CD1687 antibodies**. **a.** Biofilm formation of the 630*Δerm* strain was assayed 48h in BHISG with DCA (240µM) cultures in presence of different concentration of anti-CD1687 rabbit antibodies (0.05mg/mL to 0.2mg/mL). **b.** Growth kinetics ($OD_{600nm}$) of the WT (630*Δerm*) in BHISG medium with PBS or DCA supplemented with different concentrations of anti-CD1687 rabbit antibodies (0.05mg/mL to 0.2mg/mL). Ab: antibody; nsAb: non-specific antibody. **c**. The alphafold2 predicted structure of CD1687 show a N-terminal signal peptide S (red) connected to the α beta domain (purple) by a linker peptide (green), with another similar β beta domain (yellow) in the C-terminal region. **d**. 48h biofilms form by various *Δ1687* strain complemented with an empty vector (pDIA6103) or plasmids overexpressing the full length CD1687 (pDIA6920) or truncated CD1687 lacking either one of the two domains removed (pDIA7242 and pDIA7243, Table S1) grown in BHISG with ATC (100ng/mL) and DCA (240µM). Each data point represents an independent biological replicate composed of 2 to 4 technical replicates. Asterisks indicate statistical significance with a one-way ANOVA test followed by Dunnett's multiple comparison test (a) (ns: not significant;**: $p<0.01$) or a Tukey's multiple comparison test (d) (ns: not significant;****: $p<0.001$).

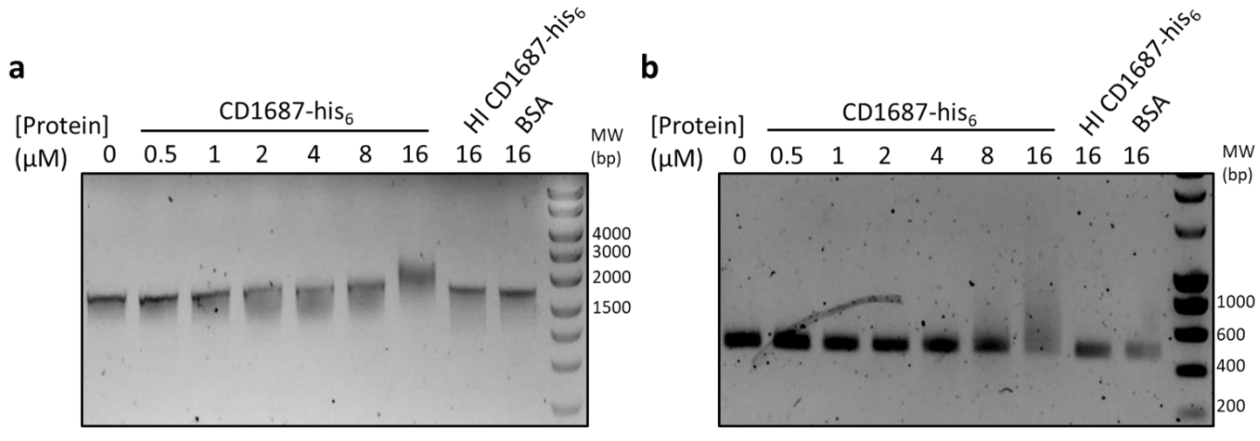


**Figure 6: CD1687 binds DNA and shifts DNA migration.** Electrophoretic Mobility shift assay (EMSA) was performed with **a.** *E. coli* plasmid pUC9 or **b.** *C. difficile* DNA (450bp PCR-amplicon) mixed with various concentrations of CD1687 (up to 16µM), with 16µM of heat inactivated (HI) CD1687 or BSA used as controls.